Supplementary information

Future Atlantic Meridional Overturning Circulation weakening driven by Labrador Sea warming and salt transport feedback

Won-Il Lim[1], Hyo-Seok Park[1*] and Andrew Stewart[2]

[1]*Department of Ocean Science and Technology, Hanyang University, Ansan, South Korea*

[2]*Department of Atmospheric and Oceanic Sciences, University of California, Los Angeles, USA*

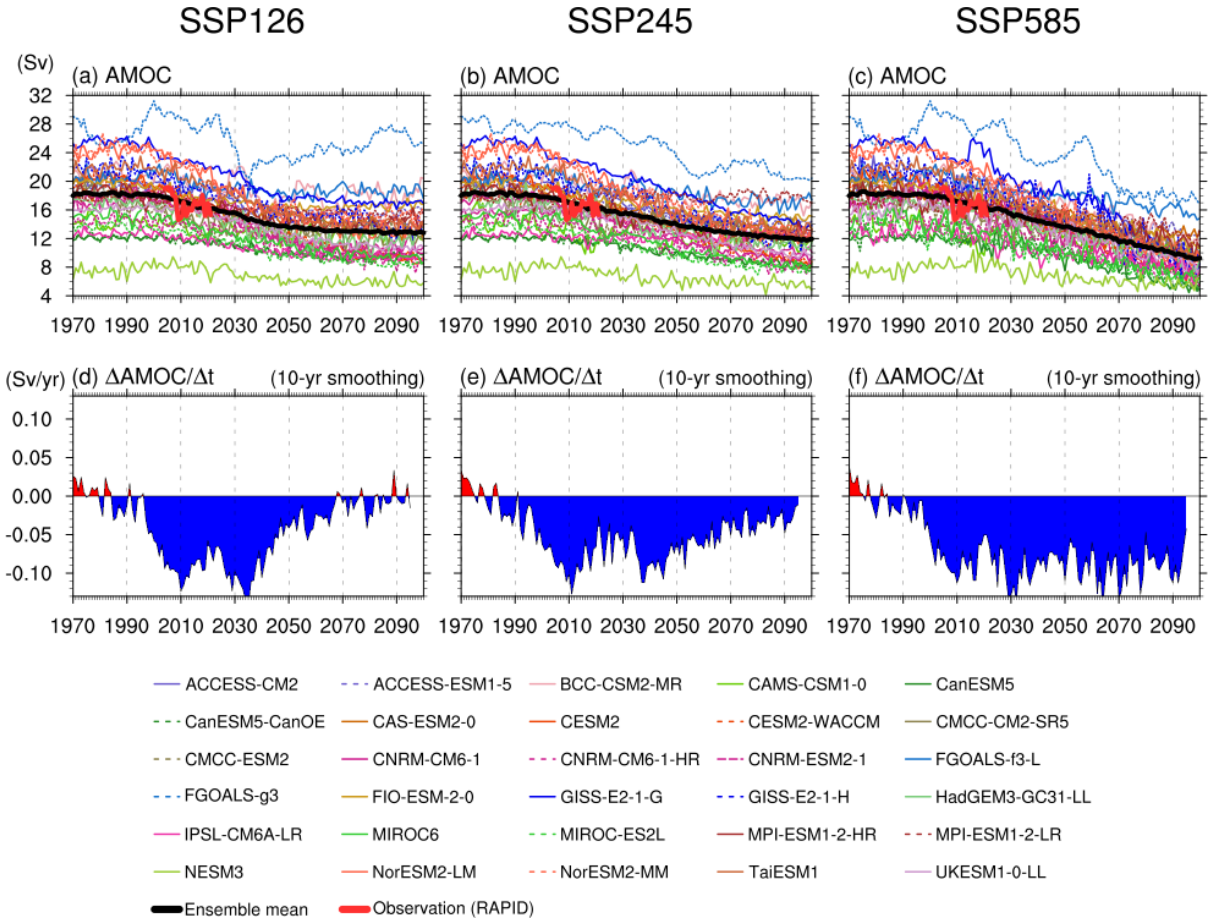

Supplementary Figure 1: AMOC strength and interannual change rate.

The annual-mean AMOC strength and the rate of AMOC change spanning 1850 to 2100. The top panel shows the AMOC strength derived from CMIP6 simulations under three scenarios: **(a)** Historical + SSP-126, **(b)** Historical + SSP-245, and **(c)** Historical + SSP-585, alongside RAPID observations from 2004 to 2021 (red line). The bottom panel shows the AMOC change rate (ΔAMOC/year) from CMIP6 simulations under the same scenarios: **(d)** Historical + SSP-126, **(e)** Historical + SSP-245, and **(f)** Historical + SSP-585. In the bottom panel, red (blue) shading indicates a positive (negative) AMOC change rate.

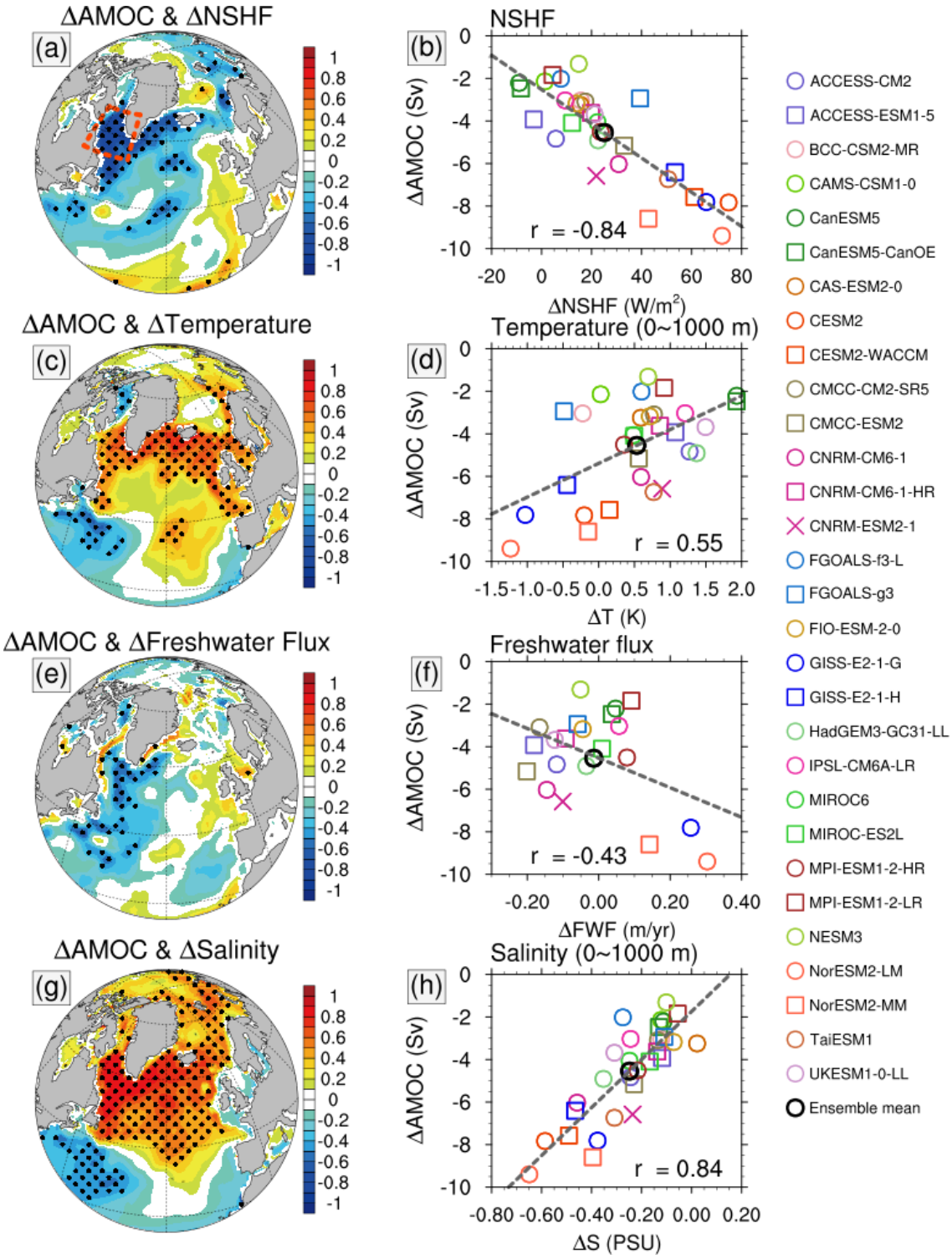

Supplementary Figure 2: Multi-model relationship between AMOC changes and surface flux changes Historical and SSP-126 scenario simulations

(a, c, e, g) Correlation map: inter-model correlations between **(a)** ΔAMOC and ΔNSHF, **(c)** ΔAMOC and ΔT (0–1000m temperature average), **(e)** ΔAMOC and ΔFWF (freshwater flux),

and **(g)** ΔAMOC and ΔS (0–1000m salinity average), at each grid cell. Here, Δ implies the temporal change from 1990 to 2050. It correlates the differences in ΔAMOC across models with the inter-model differences in ΔNSHF, ΔFreshwater flux, ΔTemperature, and ΔSalinity at each grid cell. **(b, d, f, h)** Multi-model correlation between **(b)** ΔAMOC and ΔNSHF, **(d)** ΔAMOC and ΔT, **(f)** ΔAMOC and ΔFWF, and **(h)** ΔAMOC and ΔS, averaged over the Labrador Sea (ornage dotted line in **(a)**) in Historical and SSP-126 scenario simulations**.** The gray-dashed lines in **(b, d, f, h)** indicate the regression lines of the multi-models.

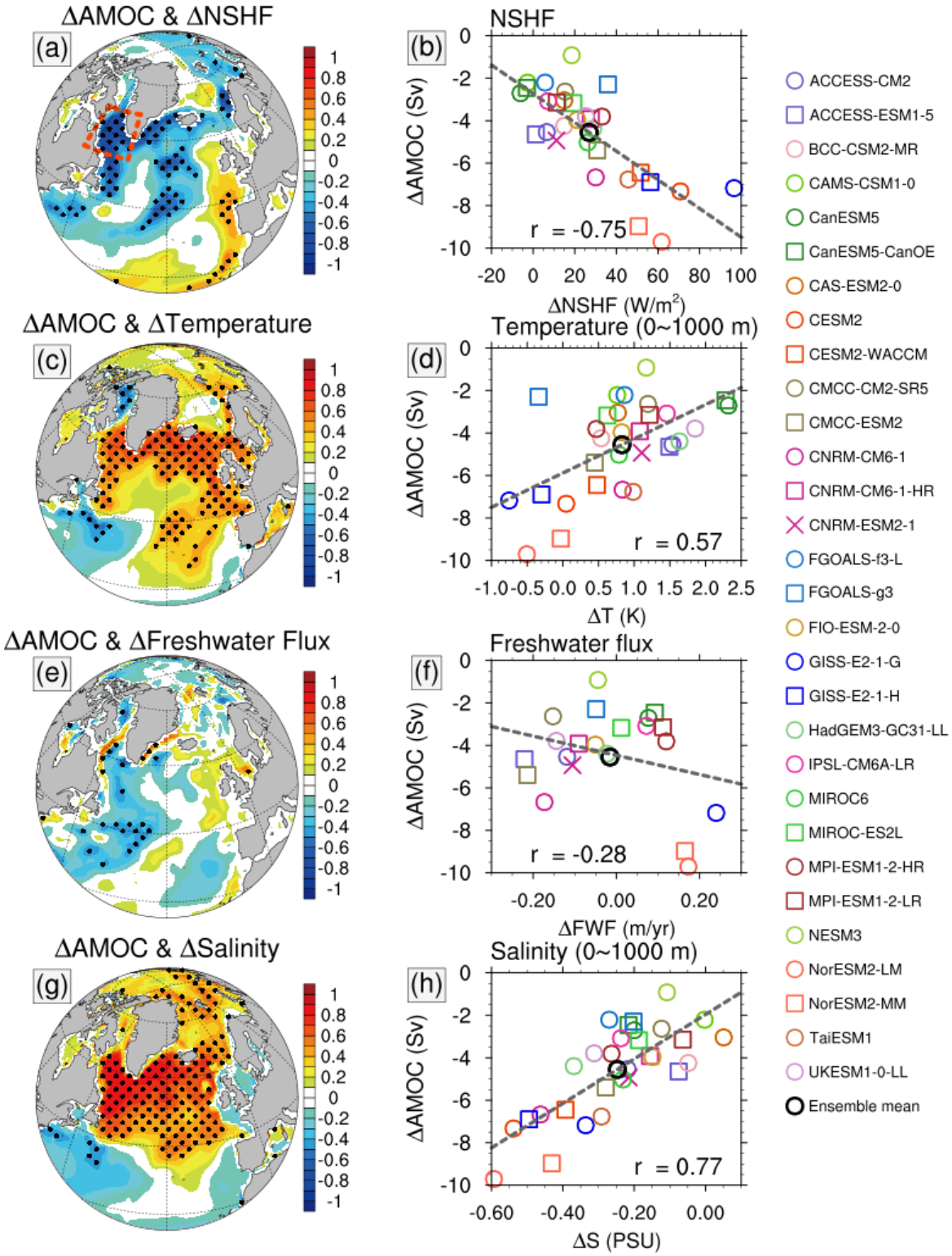

Supplementary Figure 3: Multi-model relationship between AMOC changes and surface flux changes in Historical and SSP-585 scenario simulations

Same as Supplementary Fig. 3 except for Historical and SSP-585 scenario simulations.

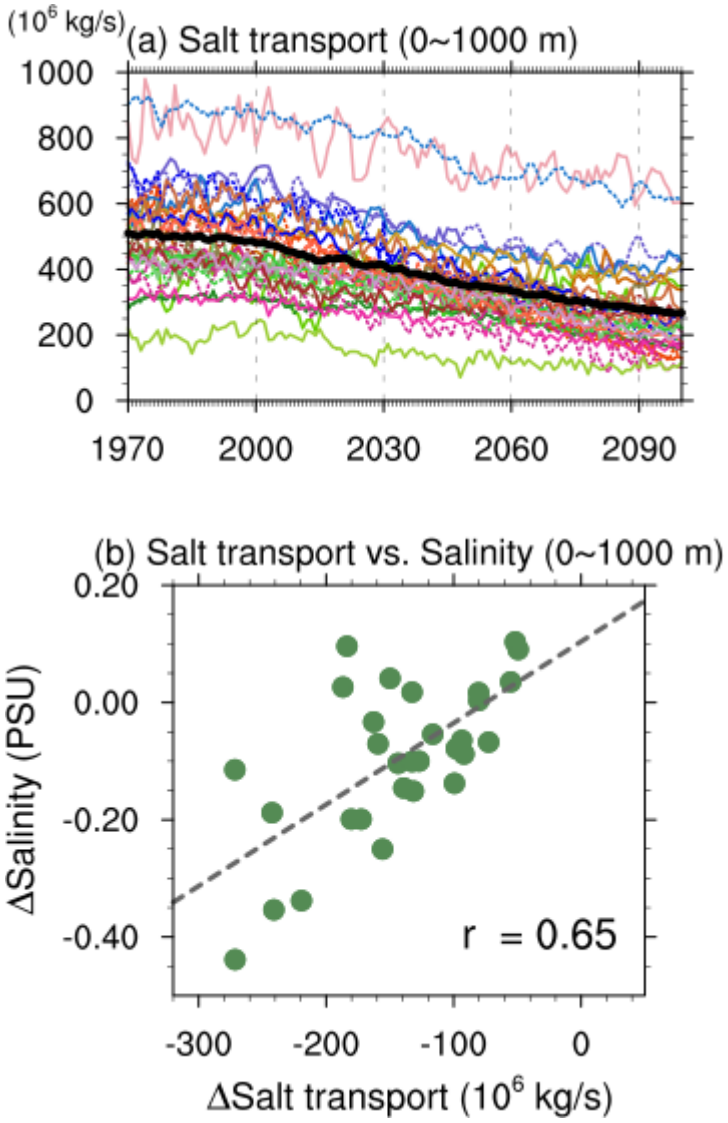

Supplementary Figure 4: Changes in meridional salt transport

(a) The CMIP6 annual-mean meridional salt transport at 50°N spanning 1970 to 2100 from CMIP6 simulations under Historical and SSP-245 scenarios. **(b)** Multi-model correlations between ΔSalt transport and ΔSalinity (0–1000 m average), averaged in the Labrador Sea in Historical and SSP-245 scenario simulations. Here, Δ implies the temporal change from 1990 to 2050. The gray-dashed lines in **(b)** indicate the regression lines of the multi-models.

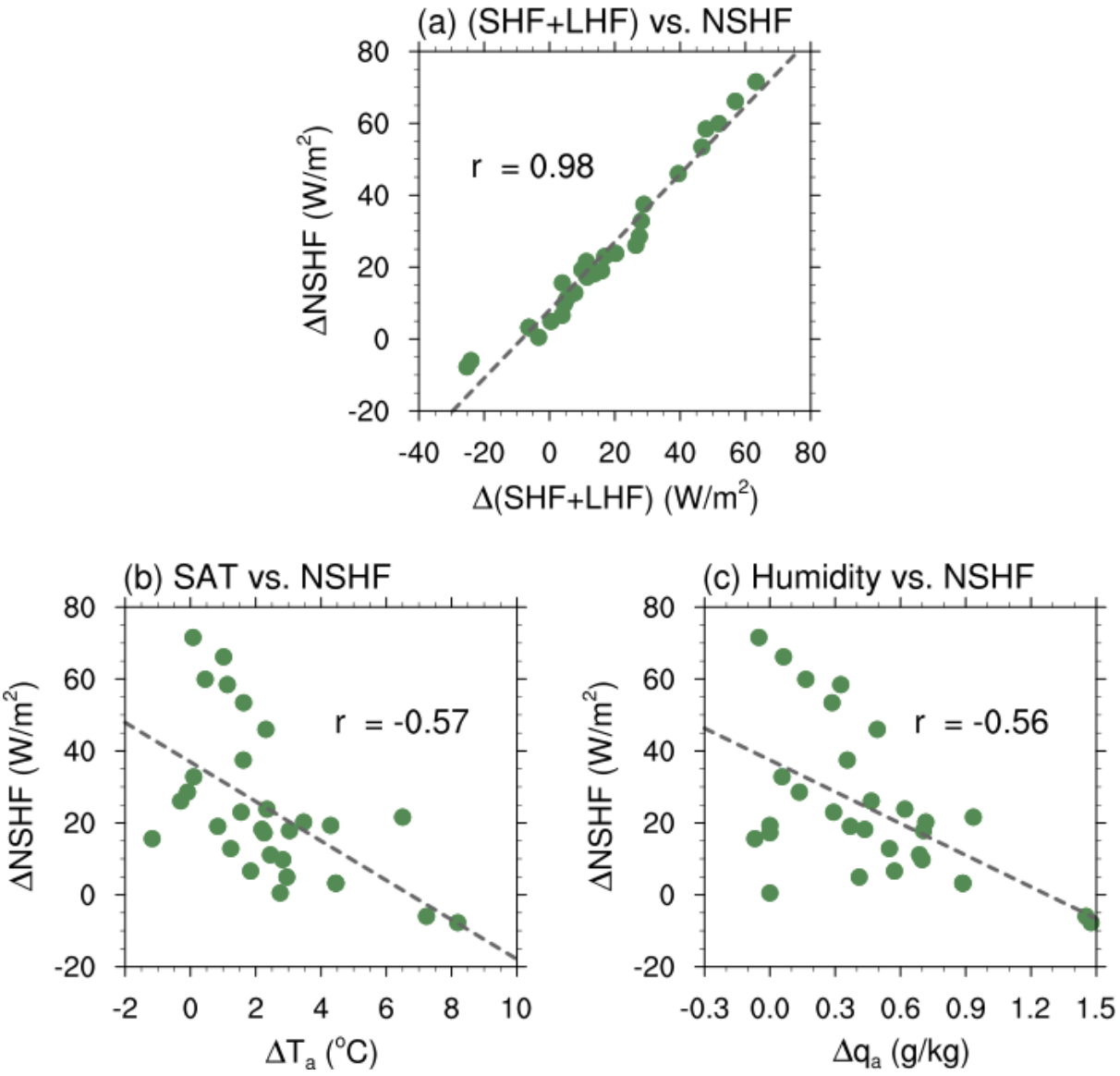

Supplementary Figure 5: Multi-model relationship between surface turbulent heat flux changes and NSHF cahnges

Multi-model correlation between **(a)** Δturbulenta heat flux (sensible + latent heat flux) and ΔNSHF, **(b)** Δ(surface air temperature) and ΔNSHF, and **(c)** Δ(surface specific humidity) and ΔNSHF, averaged over the Labrador Sea in Historical and SSP-245 scenario simulations. The gray-dashed lines indicate the regression lines of the multi-models.

Table S1. Information of CMIP6 list and member used in this study.

Model	Member	Reference
ACCESS-CM2	r1i1p1f1, r2i1p1f1, r3i1p1f1, r4i1p1f1, r5i1p1f1	ref. [1]
ACCESS-ESM1-5	r1i1p1f1, r2i1p1f1, r3i1p1f1, r4i1p1f1, r5i1p1f1	ref. [2,3]
BCC-CSM2-MR	r1i1p1f1	ref. [4]
CAMS-CSM1-0	r1i1p1f1	ref. [5]
CanESM5	r1i1p2f1, r2i1p2f1, r3i1p2f1, r4i1p2f1, r5i1p2f1	ref. [6]
CanESM5-CanOE	r1i1p2f1, r2i1p2f1, r3i1p2f1	ref. [6]
CAS-ESM2-0	r1i1p1f1, r3i1p1f1	ref. [7]
CESM2	r4i1p1f1, r10i1p1f1, r11i1p1f1	ref. [8]
CESM2-WACCM	r1i1p1f1	ref. [8]
CMCC-CM2-SR5	r1i1p1f1	ref. [9]
CMCC-ESM2	r1i1p1f1	ref. [10]
CNRM-CM6-1	r1i1p1f2, r2i1p1f2, r3i1p1f2, r4i1p1f2, r5i1p1f2	ref. [11]
CNRM-CM6-1-HR	r1i1p1f2	ref. [11]
CNRM-ESM2-1	r1i1p1f2	ref. [12]
FGOALS-f3-L	r1i1p1f1	ref. [13]
FGOALS-g3	r1i1p1f1	ref. [14]
FIO-ESM-2-0	r1i1p1f1, r2i1p1f1, r3i1p1f1	ref. [15]

GISS-E2-1-G	r1i1p1f2, r2i1p1f2, r3i1p1f2, r4i1p1f2, r5i1p1f2	ref. [16]
GISS-E2-1-H	r1i1p1f2, r2i1p1f2, r3i1p1f2, r4i1p1f2, r5i1p1f2	ref. [17]
HadGEM3-GC31-LL	r1i1p1f3	ref. [18]
IPSL-CM6A-LR	r1i1p1f1, r2i1p1f1, r3i1p1f1, r4i1p1f1, r6i1p1f1	ref. [19]
MIROC6	r1i1p1f1, r2i1p1f1, r3i1p1f1, r4i1p1f1, r5i1p1f1	ref. [20]
MIROC-ES2L	r1i1p1f2, r2i1p1f2, r3i1p1f2, r4i1p1f2, r5i1p1f2	ref. [21]
MPI-ESM1-2-HR	r1i1p1f1, r2i1p1f1	ref. [22]
MPI-ESM1-2-LR	r1i1p1f1, r2i1p1f1, r3i1p1f1, r4i1p1f1, r5i1p1f1	ref. [23]
NESM3	r1i1p1f1, r2i1p1f1	ref. [24]
NorESM2-LM	r1i1p1f1	ref. [25]
NorESM2-MM	r1i1p1f1	ref. [25]
TaiESM1	r1i1p1f1	ref. [26]
UKESM1-0-LL	r1i1p1f2, r2i1p1f2, r3i1p1f2, r4i1p1f2, r8i1p1f2	ref. [27]

References

1. Bi, D. *et al.* The ACCESS coupled model: description, control climate and evaluation. *Aust. Meteorol. Oceanogr. J.* **63**, 41–64 (2013).
2. Law, R. M. *et al.* The carbon cycle in the Australian Community Climate and Earth System Simulator (ACCESS-ESM1) – Part 1: Model description and pre-industrial simulation. *Geosci. Model Dev.* **10**, 2567–2590 (2017).
3. Ziehn, T., Lenton, A., Law, R. M., Matear, R. J. & Chamberlain, M. A. The carbon cycle in the Australian Community Climate and Earth System Simulator (ACCESS-ESM1) – Part 2: Historical simulations. *Geosci. Model Dev.* **10**, 2591–2614 (2017).
4. Wu, T. *et al.* The Beijing Climate Center Climate System Model (BCC-CSM): the main progress from CMIP5 to CMIP6. *Geosci. Model Dev.* **12**, 1573–1600 (2019).
5. Rong, X. *et al.* The CMIP6 Historical Simulation Datasets Produced by the Climate System Model CAMS-CSM. *Adv. Atmospheric Sci.* **38**, 285–295 (2021).
6. Swart, N. C. *et al.* The Canadian Earth System Model version 5 (CanESM5.0.3). *Geosci. Model Dev.* **12**, 4823–4873 (2019).
7. Zhang, H. *et al.* Description and Climate Simulation Performance of CAS-ESM Version 2. *J. Adv. Model. Earth Syst.* **12**, e2020MS002210 (2020).
8. Danabasoglu, G. *et al.* The Community Earth System Model Version 2 (CESM2). *J. Adv. Model. Earth Syst.* **12**, e2019MS001916 (2020).
9. Cherchi, A. *et al.* Global Mean Climate and Main Patterns of Variability in the CMCC-CM2 Coupled Model. *J. Adv. Model. Earth Syst.* **11**, 185–209 (2019).
10. Lovato, T. *et al.* CMIP6 Simulations With the CMCC Earth System Model (CMCC-ESM2). *J. Adv. Model. Earth Syst.* **14**, e2021MS002814 (2022).
11. Voldoire, A. *et al.* Evaluation of CMIP6 DECK Experiments With CNRM-CM6-1. *J. Adv.*

Model. Earth Syst. **11**, 2177–2213 (2019).

12. Séférian, R. *et al.* Evaluation of CNRM Earth System Model, CNRM-ESM2-1: Role of Earth System Processes in Present-Day and Future Climate. *J. Adv. Model. Earth Syst.* **11**, 4182–4227 (2019).
13. He, B. *et al.* CAS FGOALS-f3-L Model Datasets for CMIP6 Historical Atmospheric Model Intercomparison Project Simulation. *Adv. Atmospheric Sci.* **36**, 771–778 (2019).
14. Li, L. *et al.* The Flexible Global Ocean-Atmosphere-Land System Model Grid-Point Version 3 (FGOALS-g3): Description and Evaluation. *J. Adv. Model. Earth Syst.* **12**, e2019MS002012 (2020).
15. Bao, Y., Song, Z. & Qiao, F. FIO-ESM Version 2.0: Model Description and Evaluation. *J. Geophys. Res. Oceans* **125**, e2019JC016036 (2020).
16. Schmidt, G. A. *et al.* Configuration and assessment of the GISS ModelE2 contributions to the CMIP5 archive. *J. Adv. Model. Earth Syst.* **6**, 141–184 (2014).
17. Kelley, M. *et al.* GISS-E2.1: Configurations and Climatology. *J. Adv. Model. Earth Syst.* **12**, e2019MS002025 (2020).
18. Kuhlbrodt, T. *et al.* The Low-Resolution Version of HadGEM3 GC3.1: Development and Evaluation for Global Climate. *J. Adv. Model. Earth Syst.* **10**, 2865–2888 (2018).
19. Dufresne, J.-L. *et al.* Climate change projections using the IPSL-CM5 Earth System Model: from CMIP3 to CMIP5. *Clim. Dyn.* **40**, 2123–2165 (2013).
20. Tatebe, H. *et al.* Description and basic evaluation of simulated mean state, internal variability, and climate sensitivity in MIROC6. *Geosci. Model Dev.* **12**, 2727–2765 (2019).
21. Hajima, T. *et al.* Development of the MIROC-ES2L Earth system model and the evaluation of biogeochemical processes and feedbacks. *Geosci. Model Dev.* **13**, 2197–2244 (2020).
22. Müller, W. A. *et al.* A Higher-resolution Version of the Max Planck Institute Earth System

Model (MPI-ESM1.2-HR). *J. Adv. Model. Earth Syst.* **10**, 1383–1413 (2018).

23. Mauritsen, T. *et al.* Developments in the MPI-M Earth System Model version 1.2 (MPI-ESM1.2) and Its Response to Increasing CO2. *J. Adv. Model. Earth Syst.* **11**, 998–1038 (2019).
24. Cao, J. *et al.* The NUIST Earth System Model (NESM) version 3: description and preliminary evaluation. *Geosci. Model Dev.* **11**, 2975–2993 (2018).
25. Seland, Ø. *et al.* Overview of the Norwegian Earth System Model (NorESM2) and key climate response of CMIP6 DECK, historical, and scenario simulations. *Geosci. Model Dev.* **13**, 6165–6200 (2020).
26. Lee, W.-L. *et al.* Taiwan Earth System Model Version 1: description and evaluation of mean state. *Geosci. Model Dev.* **13**, 3887–3904 (2020).
27. Sellar, A. A. *et al.* UKESM1: Description and Evaluation of the U.K. Earth System Model. *J. Adv. Model. Earth Syst.* **11**, 4513–4558 (2019).